Journal of the Ghana Institution of Engineering (2023) 23:1
https://doi.org/10.56049/jghie.v23i1.64

ORIGINAL RESEARCH

Analysis and prediction of land use land cover dynamics in the Kpeshie Lagoon Basin of Ghana using satellite remote sensing

Yaw Mensah Asare[1,*], Irving Selby[2], George Ashiagbor[3], Cosmas Yaw Asante[1]

Received: 10th October, 2022 / **Accepted:** 14th January, 2023
Published online: 3rd March, 2023

Abstract

Accurate and current Land Use and Land Cover (LULC) maps are important for planning purposes and to monitor the alterations to the environment mostly caused by humans activities. The increased utilization of land resources due to population growth have led to loss of biodiversity and urban planning issues such as flooding and pollution. This study analysed LULC changes over the Kpeshie lagoon Basin of the Greater Accra Region of Ghana and made prediction to the year 2030. Random Forest (RF) classifier was employed to classify the LULC over the study area using Landsat image for four different time-steps (1991, 2002, 2013 and 2020). LULC change analysis was performed for consecutive years (1991 – 2002, 2002 – 2013 and 2013 – 2020) and for the entire period (1991 – 2020). Subsequently, a prediction of LULC was done the year 2030 using a combination of artificial neural network (ANN) and cellular automata (CA) simulations. The LULC classification produced 92.68 %, 84.35 %, 84.41 % and 89.93 % overall accuracies and kappa statistics of 0.87, 0.87, 0.84 and 0.91 for the time-steps respectively. Over the study period, significant LULC changes were observed, as the Kpeshie Lagoon Basin which was predominantly covered by vegetation (69.33 %) in 1991 had transformed into a major built-up area (50.50 %) in 2020. The spatial prediction estimated built-up covers 60.15 % in 2030, followed by bare land (32.39 %), vegetation (6.97 %) and waterbody (0.49 %). The study revealed that LULC within the Kpeshie Lagoon Basin has been immensely impacted due to urbanization and non-enforcement of regulations. Continuation of the current LULC trend, where vegetation and waterbody decrease while built-up area increases would make the Kpeshie Lagoon basin vulnerable to the challenges of climate change.

Keywords: Land Use and Land Cover, Random Forest, LULC Change, Satellite Image, Landsat

Introduction

Historically, land cover on the earth's surface has seen significant changes (Dewan and Yamaguhi, 2009). There are both natural (volcanic eruptions, tsunamis, earthquakes, etc) and human-induced causes attributed to these changes. Utilisation of land resources by humans for residential and socio-economic activities has been the main cause of land cover changes (Yadav *et al*., 2012). Land Use and Land Cover (LULC) changes have led to the loss of biodiversity (OECD, 2019) which has been influenced by increasing population, urbanisation, forest conversion and agricultural expansion (Zurqani *et al*., 2018). However, effective spatial planning can control these LULC changes to protect biodiversity while catering for the needs of humans.

Accurate and up-to-date LULC maps are important inputs to biophysical and environmental assessment models required for decision-making and resource planning (Forkuor *et al*., 2017a). The utilisation of land resources by humans for residential and socio-economic activities have been the main cause of land cover changes (Yadav *et al*., 2012). LULC changes have led to the loss of biodiversity, which is most driven by increasing population (Zurqani *et al*., 2018).

*Corresponding author's email: mensah.yasare@gmail.com

[1]Department of Geomatic Engineering, Kwame Nkrumah University of Science and Technology, Kumasi, KNUST, Kumasi-Ghana.

[2] Land Use and Spatial Planning Authority (LUSPA), Central Region Directorate, Cape Coast, Ghana.

[3] Faculty of Renewable Natural Resources (FRNR), Kwame Nkrumah University of Science and Technology (KNUST), Kumasi, Ghana.

Water covers 71 % of the earth surface out of which 97 % is the ocean. Fresh water (rivers, lakes and lagoons) constitutes 0.5 % of the earth surface and has been under the threat of human activities. Globally, an area of 244,000 km^2 has been converted to built-up areas and 90,000 km^2 of surface water has been lost (OECD, 2019). In West Africa, degraded forest, and gallery forest (that is, forest that forms as corridors along waterbodies) had a total net loss of 100,176 km^2, or 24.6 % from 1975 to 2013, mainly to human settlements (Cotillon, 2017).

From 1950 to 2021, the population of Ghana has grown from about 5 million to 30.8 million (Ghana Statistical Service, 2021), with a projection of upto 52 million in the year 2050 (United Nations Population Division, 2019). The expansive growth of population in Ghana is heavily impacting the natural environment, LULC changes, are particularly linked to expansion in agriculture and urban areas (Coulter *et al*., 2016). Studies that assess the dynamics of LULC and its impacts are important for taking remedial measures and planning to protect the environment whiles catering for the needs of humans. LULC data are critical variables for studies in climate change, performance of ecosystem, hydrologic and atmospheric models (Gong *et al*., 2013).

Despite the high diversity and dynamic of LULC in Ghana, the country lacks accurate and up-to-date information on LULC, which is essential to appropriately monitor changes and assess their impacts (Esteve *et al*., 1998; Forkuor *et al*., 2014; Poorter *et al*., 2004). This has resulted in the inability of governments to clampdown on activities which are degrading the environment such as illegal small-scale mining and indiscriminate timber logging (Merem *et al*., 2017; Tom-Dery *et al*., 2012). It is therefore important for researchers to provide current and timely geo-spatial information on LULC for sustainable development.

Currently, earth observation systems' data undisputedly is the most efficient and widely used data for monitoring, evaluation and assessment of land features and changes because of its ability to produce consistent and comprehensive data both in time and space (Forkuor *et al*., 2017b). Earth observation data particularly, optical images has been extensively used in LULC studies and applications because of its availability (Ghansah *et al*., 2016; Lunetta *et al*., 2006; Vittek *et al*., 2014).

The most popular optical satellite images are from the Landsat series, which started way back in 1972 (Loveland and Dwyer, 2012) and has been used in many terrestrial research ranging from agriculture (Leslie *et al*., 2017; Stefanski *et al*., 2014; Torbick *et al*., 2017), forest (Onojeghuo and Onojeghuo, 2015; White *et al*., 2017), soil (Aksoy *et al*., 2009; Azabdaftari and Sunar, 2016; Nawar *et al*., 2014), water (Hellweger *et al*., 2004; Laili *et al*., 2015), and human settlements (Hu *et al*., 2016; Lu *et al*., 2008), among others. The datasets, which are stored in the United States Geological Surveys (USGS) database, can be downloaded free of charge via internet from any part of the world (Roy *et al*., 2017). However, issues of cloud and cloud shadow cover especially in tropical regions and errors in some of the data (Landsat 7 SLC-off images) still remains a challenge (Asare *et al*., 2020) for acquiring the needed data for LULC classification.

Recent methods in LULC classification employ pixel-based image classification using spectral and/or textural properties are frequently applied to extract LULC information (Hu *et al*., 2016). Classification algorithms such as maximum likelihood, k-means and decision tree have given way to machine learning classifiers such as random forest (RF), stochastic gradient boosting (SGB) and support vector machines (SVM) (Breiman, 2001; Friedman, 2002; Mountrakis *et al*., 2011).

Rapid urbanisation has caused waterbodies to suffer immensely (EEA, 2008) especially in urban centres. Human pressures on land resources have influenced land use changes, which has impacted on waterbodies (Ayivor and Gordon, 2012). In Ghana, it can be observed that some waterbodies within urban areas are virtually non-existent while others have diminished into gutters and storm drains. Poor management of water resources, uncontrolled urbanisation and residential development in flood-prone areas are causes of flooding in Accra (Amoako and Boamah, 2015). Studies within the Kpeshie Lagoon have delved into water quality (Apau *et al.*, 2012), sanitation (Quarshie, 2015) and the influence of the Kpeshie Lagoon on flooding (Amoako and Boamah, 2015).

In the Kpeshie lagoon basin where this study was undertaken, the availability of a comprehensive information on LULC changes remains a challenge. Although several studies (Coulter *et al*., 2016; Yeboah *et al*., 2017) have used satellite data to identify LULC changes in the Greater Accra Region, most of them focused on large areas (across basins), making it difficult to capture the small changes that occur within some important basins. The present study aims at analysing the LULC changes within the Kpeshie Lagoon Basin over the last 3 decades (1991 - 2020) using Landsat images. Specifically, LULC maps were produced for four time-steps (2001, 2002, 2013 and 2020). The rate of LULC change was also determined. Finally, a prediction was made to the year 2030 for the purposes of interventions. This study is relevant because the area has gone through rapid urbanization within the last three decades. The basin is characterized by prominent features, high class residential and commercial facilities and it is a high security zone in the Greater Accra Region.

Materials and Method

Study area

Kpeshie Lagoon Basin is located in the Greater Accra Region of Ghana between latitude 5.55° to 5.68° North and longitudes 0.10° to 0.19° West with a land area of about 57.34 km^2 (Figure 1). The basin lies within the capital of Ghana, Accra (administrative and commercial hub). The area is mostly urban. Other LULC within the basin include, waterbodies (lagoon and rivers), vegetation (vegetable crop farms, open woodland, mangroves and parks/gardens) and sandy beach. The built-up areas comprise of high-class residential communities (East Legon, Spintex and Cantonment), commercial, educational and recreational facilities.

Mangroves, comprising of two dominant species (Rhizophora and Avicennia) and salt tolerant grass species are found around the Kpeshie lagoon and the tidal zone of the estuaries (Boampong, 2020). The soil is mostly infertile for crop production, but there are pockets of small-scale agricultural activities where farmers mostly grow vegetables and fruits for both consumption and commercial purposes. The northern part of the basin is covered by Savannah grass with scattered Neem trees (Ghana Statistical Service, 2014).

The geology of the basin is broadly made up of Precambrian Dahomeyan schists, granodiorites, granites gneiss and amphibolites to late precambrian togo series comprising mainly quartzite, phillites, phylitones and quartz breccias. The entire basin is underlain by Precambrian rocks of the Dahomeyan formation. The coastline of the basin has a series of resistant rock outcrops, platforms and sandy beaches near the mouth of the Kpeshie lagoon (Boampong, 2020).

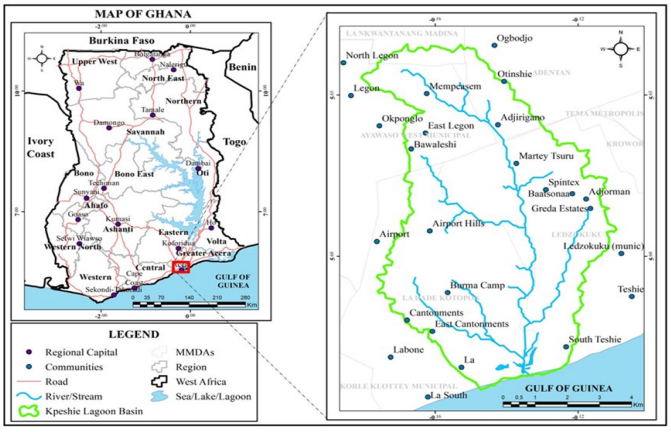

Figure 1 Map of study area

Materials, data and pre-processing

The materials used for the study has been grouped into data and softwares for processing as shown in Table 1. The Landsat images and Shuttle Radar Topograhy Mission (SRTM) Digital Elevation Model (DEM) used in this study were obtained from the United States Geological Survey (USGS) Earth Explorer; the study area falls within path 193 and row 056 with the worldwide Reference System (WRS). Due to the span of the study, the satellite images were acquired from different Landsat sensors (Table 2). All the Landsat images used were collection-2 level-2 (C2L2) surface reflectance product; that is, they have been atmospherically corrected. Image-to-image registration were performed to ensure the alignment of corresponding pixels.

The scanline errors in the 2013 Landsat 7 EMT$^+$ images were corrected through a gap-filling process (Asare *et al*., 2020). The gap-filling process was done using Exellis ENVI 5.0. The Landsat images and DEM were at a resolution of 30m. The DEM used for the hydrologic analysis was acquired on 11th November 2010.

Table 1 Materials for the study

Data	Software
i. Landsat Satellite Imagery (1991, 2002, 2013 and 2020) ii. Shuttle Radar Topograhy Mission (STRM) Digital Elevation Model (DEM) iii. Training and Validation Data	i) ESRI ArcGIS 10.5 (ArcMap) ii) Exellis ENVI 5.0 iii) QGIS 2.18 iv) Microsoft Excel 2016 v) Google Earth Engine (GEE)

Table 2 Landsat used for the study

Image ID	Satellite	Sensor	Acquisition Date
LT41930561991010XXX03	Landsat 5	Thematic Mapper (TM)	10-01-1991
LE71930562002360EDC00	Landsat 7	Enhanced Thematic Mapper (ETM+)	26-12-2002
LE71930562013358ASN00	Landsat 7	Enhanced Thematic Mapper (ETM+)	24-12-2013
LC81930562020226LGN00	Landsat 8	Operational Land Imager (OLI) Thermal Infrared Sensor (TIRS)	13-08-2020

Table 3 Training and validation data for LULC classes

LULC Class	Training	%	Validation	%	Total	%
Built-up	45	32.14	20	33.33	65	32.50
Vegetation	45	32.14	20	33.33	65	32.50
Bare land	35	25.00	10	16.67	45	22.50
Waterbody	15	10.72	10	16.67	25	12.50
Total	**140**	**100**	**60**	**100**	**200**	**100**

For the purpose of classification, training/validation data for the years were obtained from google earth engine, existing maps and through field visits. For this study, four main LULC types (Built-up, Bare land, waterbody and vegetation) were identified in the study area. A total of 200 Ground Control Points (GCPs) were taken, 140 (70 %) for training and the other 60 (30 %) for validation.

Method

Delineation of study basin

The boundary of the Kpeshie Lagoon Basin was delineated using the DEM to show the catchment area for the study. The process was carried out using the spatial analyst tool in ArcMap 10.5 software. Before the delineating process began, an estimated size of the DEM covering a wider area than the Kpeshie Lagoon Basin was sub-set using the '*Clip*' tool in the '*Image Analyst*' package in Arc Map 10.5 software. The sub-set DEM was filled to remove the sinks to ensure proper delineation of the basin as it will avoid the drainage network from being discontinuous. The flow direction and accumulation were then derived, after which the watershed (basin) within the interest area was delineated. The output raster image was then converted into a polygon shapefile to describe the extent of the study area.

Image classification and accuracy assessment

Supervised Image classification was done using a non-parametric Random Forest (RF) classification algorithm (Breiman, 2001). RF belongs to the family of ensemble machine learning algorithms that predicts a response from a set of predictors by creating multiple Decision Trees (DTs) and aggregating their results. Each tree in the forest is independently constructed using a unique bootstrap sample of the training (Forkuor *et al*., 2017b). The advantage of RF over the other machine learning algorithms is its ability to choose the best split from a randomly selected sub- set of predictors (Breiman, 2001). The training data obtained from Google Earth Engine (GEE), existing maps and field visit aided in the selection of ground truth points of the various LULC types (for each year) to train the RF classifier. The training/validation data were split into 70% training and 30 % validation using a stratified random sampling approach. The number of GCPs for each LULC class is shown in Table 3. In running the algorithm, the number of trees (ntrees) was set to 500 and the number of predictors to be tried (ntry) set at 5.

To assess the performance of the RF classifier, the independent 30 % validation data were used. A confusion matrix which provides information on the correct and incorrect prediction made by a classification algorithm by comparing a classified map with ground information was used in calculating the overall accuracy (OA) and the kappa (k) statistics. The OA is the ratio of correctly classified pixels to all pixels considered in the evaluation, whereas k measures the agreement between the classification by assessing if there is a significant difference between the confusion matrix and a random result (Congalton, 1991; Smits *et al*., 1999).

Post-classification analysis and change detection

Based on the classified LULC maps (1991, 2002, 2013 and 2020), LULC statistics were computed for all the LULC classes. Furthermore, statistics of changes in LULC between years (1991-2002, 2002-2013, 2013-2020 and 1991-2020) and their corresponding change maps were generated and analysed. The analysis gave values of LULC area distribiution for each time-step and estimates of change between two time-steps. In the change analysis, the idea is to identify what has change 'from' – 'to'. This will produce a change matrix to track the trajectories of each pixel between two time-steps to determine the trade-offs between the LULC classes within the basin.

The rate of change was then determined considering the number of years between the consecutive years and the corresponding land area change. The formula (Equation 1) was adopted for determining the rate of change for the consecutive time-steps and then the entire study period.

$$Rate\ of\ change = \left[(a_2 \div a_1)^{1/n} - 1\right] \times 100 \qquad (1)$$

Where a_1 *and* a_2 are the start and end years data respectively and n is the number of years (Pandit, 2011).

Spatial prediction

Based on the LULC trends from 1991 to 2020, future LULC was predicted to the year 2030. A QGIS version 2.0 plugin '*MOLUSCE*' (Modules of Land Use Change Simulations) developed by NextGIS (NextGIS, 2013) was used for the spatial prediction. In the spatial prediction process, the MOLUSCE tool analyses the statistics of changes between land -use classes and simulates the 'change map' using artificial neural network (ANN). Subsequently, with the change map as an input, a cellular automata (CA) simulation was carried out to predict a LULC map for the year 2030. Before the prediction to the year 2030, the model was validated with the LULC map of 2020. The detailed process carried out in the spatial prediction to obtain the predicted LULC map can be found in (Aneesha *et al*., 2020; Kamaraj and Rangarajan, 2022).

Results

Classified land use/land cover

Land use/cover within the Kpeshie Lagoon Basin changed over the study period (Figure 2). Vegetation covered majority of the total land area within the basin in 1991 and 2002, that is, a total land area of 39.754 km^2 (69.33 %) and 21.284 km^2 (37.12 %) respectively. Built-up covered almost half (48.86 %) of the total land area in 2013 and half (50.50%) in 2020, that is, land areas of 28.013 km^2 and 28.957 km^2 respectively. Waterbody was the least land cover throughout the study period covering land areas of 0.744 km^2 (1.30 %) in 1991, 0.350 km^2 (0.61 %) in 2002, 0.342 km^2 (0.60 %) in 2013 and 0.340 km^2 (0.59 %) in 2020. The details of land area for each LULC class and their proportions (Table 4).

Accuracy assessment of image classification

Accuracy of the LULC classification for all (1991, 2002, 2013 and 2020) satellite images were assessed using the error (confusion) matrix. The overall accuracy for 1991, 2002, 2013 and 2020 classification were 92.68 %, 84.35 %, 84.41 % and 89.93 % and the kappa statistics were 0.87, 0.87, 0.84 and 0.91 respectively.

LULC change analysis

LULC change analysis was done to determine the land cover changes between the years. Figure 3 shows the spatial distribution map of the change analysis of LULC for the consecutive time-steps and the entire period. Tables 5 – 8 show the details of the change analysis for the time-steps.

From 1991 to 2002 (Table 5), a total land area of 25.129 km^2 (43.82 %) remained unchanged. Built-up maintained almost half (49.98 %) of its land area, that is, 4.341 km^2. Vegetation maintained the highest land area, that is, 17.189 km^2 while waterbody was the least representing 0.320 km^2. Most (34.22 %) vegetation cover were converted to built-up representing a total land area of 13.605 km^2. The least LULC trade-off was between built-up to waterbody as only 0.007 km^2 (0.08 %) of waterbody was converted to built-up. Overall, bare land gained the most land area, that is, 11.221 km^2, a percentage change of 137.6 % while vegetation lost the most land area, that is, 18.470 km^2, a percentage change of 46.46%. Built-up experienced an increase in land area from by 7.643 km^2, a percentage change of 88 %. More than half (52.96 %) of waterbody land area was lost representing 0.394 km^2.

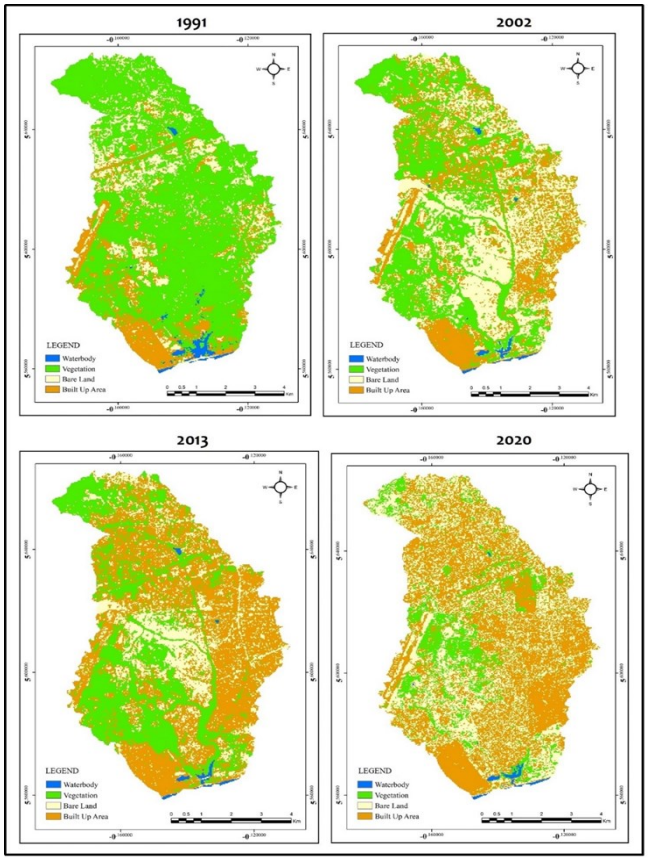

Figure 2 Classified land use/cover of Kpeshie lagoon basin

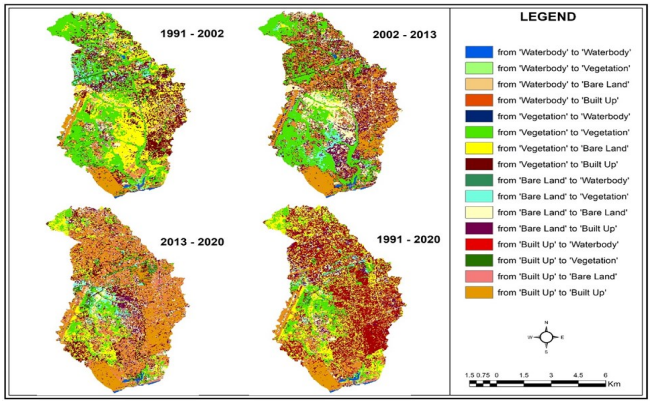

Figure 3 LULC Conversions within Kpeshie lagoon basin

Table 4 Summary of land area of LULC for the various time-steps

LULC Class	1991		2002		2013		2020	
	Area (km^2)	%	Area (km^2)	%	Area (km^2)	%	Area (km^2)	%
Waterbody	0.744	1.30	0.350	0.61	0.342	0.60	0.340	0.59
Vegetation	39.754	69.33	21.284	37.12	17.639	30.76	8.014	13.98
Bare Land	8.155	14.22	19.376	33.79	11.344	19.78	20.027	34.93
Built-Up	8.685	15.15	16.328	28.48	28.013	48.86	28.957	50.50
Total	**57.338**	**100.00**	**57.338**	**100.00**	**57.338**	**100.00**	**57.338**	**100.00**

Table 5 LULC conversion from 1991 to 2002

	LULC Class	1991 Waterbody		Vegetation		Bare land		Built-up		2002 Total
		(km^2)	%	(km^2)	%	(km^2)	%	(km^2)	%	(km^2)
	Waterbody	**0.320**	**42.93**	0.015	0.04	0.008	0.10	0.007	0.08	**0.350**
	Vegetation	0.293	39.42	**17.189**	**43.24**	1.895	23.24	1.907	21.96	**21.284**
2002	**Bare land**	0.062	8.34	13.605	34.22	**3.279**	**40.21**	2.430	27.98	**19.376**
	Built-up	0.069	9.31	8.945	22.50	2.973	36.45	**4.341**	**49.98**	**16.328**
	1991 Total	**0.744**	**100.00**	**39.754**	**100.00**	**8.155**	**100.00**	**8.685**	**100.00**	**57.338**
Total LULC Change		**-0.394**	**-52.96**	**-18.470**	**-46.46**	**11.221**	**137.60**	**7.643**	**88.00**	
Total Unchanged LULC		**25.129 km^2 (43.82%)**								

Table 6 LULC conversion from 2002 to 2013

	LULC Class	2002 Waterbody		Vegetation		Bare land		Built-up		2013 Total
		(km^2)	%	(km^2)	%	(km^2)	%	(km^2)	%	(km^2)
	Waterbody	**0.304**	**86.89**	0.005	0.02	0.014	0.07	0.019	0.12	**0.342**
	Vegetation	0.004	1.03	**14.877**	**69.85**	2.210	11.40	0.558	3.42	**17.639**
2013	**Bare land**	0.016	4.63	1.178	5.54	**7.794**	**40.23**	2.356	14.42	**11.344**
	Built-up	0.026	7.45	5.234	24.59	9.358	48.30	**13.395**	**82.04**	**28.013**
	2002 Total	**0.350**	**100.00**	**21.284**	**100.00**	**19.376**	**100.00**	**16.328**	**100.00**	**57.338**
Total LULC Change		**-0.008**	**-2.31**	**-3.645**	**-17.13**	**-8.032**	**-41.46**	**11.685**	**71.57**	
Total Unchanged LULC		**36.370 km^2 (63.43%)**								

Table 7 LULC conversion from 2013 to 2020

	LULC Class	2013 Waterbody		Vegetation		Bare land		Built-up		2020 Total
		(km^2)	%	(km^2)	%	(km^2)	%	(km^2)	%	(km^2)
	Waterbody	**0.248**	**72.37**	0.050	0.29	0.009	0.08	0.033	0.12	**0.340**
	Vegetation	0.058	17.10	**4.579**	**25.96**	1.606	14.15	1.771	6.32	**8.014**
2020	**Bare land**	0.016	4.74	7.167	40.63	**4.391**	**38.71**	8.453	30.18	**20.027**
	Built-up	0.020	5.79	5.843	33.12	5.338	47.06	**17.756**	**63.38**	**28.957**
	2013 Total	**0.342**	**100.00**	**17.639**	**100.00**	**11.344**	**100.00**	**28.013**	**100.00**	**57.338**
Total LULC Change		**-0.002**	**-0.53**	**-9.625**	**-54.56**	**8.683**	**76.55**	**0.944**	**3.37**	
Total Unchanged LULC		**26.974 km^2 (35.39%)**								

Table 8 LULC Conversion from 1991 to 2020

		1991								2020 Total
	LULC Class	Waterbody		Vegetation		Bare land		Built-up		
		(km²)	%	(km²)	%	(km²)	%	(km²)	%	(km²)
2020	**Waterbody**	**0.298**	**40.03**	0.031	0.08	0.007	0.08	0.005	0.06	**0.340**
	Vegetation	0.198	26.60	**6.265**	**15.76**	0.799	9.80	0.752	8.67	**8.014**
	Bare land	0.099	13.30	14.537	36.57	**3.002**	**36.82**	2.389	27.50	**20.027**
	Built-Up	0.149	20.07	18.921	47.59	4.347	53.30	**5.539**	**63.77**	**28.957**
	1991 Total	**0.744**	**100.00**	**39.754**	**100.00**	**8.155**	**100.00**	**8.685**	**100.00**	**57.338**
Total LULC Change		**-0.404**	**-54.29**	**-31.740**	**-79.84**	**11.872**	**145.58**	**20.272**	**233.41**	
Total Unchanged LULC		**15.104 km²**								

A total land area of 38.370 km² remained unchanged from 2002 to 2013 (Table 6), representing 63.42 %. From the total unchanged land area, most (40.89 %) vegetation remained unchanged with a land area of 14.877 km² while waterbody was the least (0.01 %) with a total land area of 0.304 km². The highest land area trade-off was from bare land to built-up, that is, bare land lost a land area of 9.358 km² (48.3 %) to built-up. About a quarter (24.59 %) of vegetation land area was traded-off to built-up representing 5.234 km². In general, built-up was the only LULC class to record an increase in land area by 11.685 km², representing a percentage change of 71.57 %. All other LULC classes experienced a decrease in land area. Bare land decreased the most (41.46 %) by 8.032 km² while waterbody experienced the least (2.31 %) by 0.008 km². Vegetation decreased marginally (17.13 %) by a land area of 3.645 km².

From 2013 to 2020 (Table 7), the total unchanged land area was 26.974 km² (35.39 %). Out of the unchanged land area, most (65.83 %) built-up remained unchanged, that is, a total land area of 17.756 km² while waterbody had the least (0.01%) representing 0.248 km². Bare land gained the most from land cover conversions over the period, as built-up and vegetation lost land areas of 8.453 km² and 7.167 km² to bare land, representing 30.17 % and 40.63 % respectively. Bare land traded off a land area of 0.009 km² to waterbody, which is the least (0.08 %) trade off within the 7-year period. Overall, bare land and built-up recorded increase in land area. Bare land increased by 8.683 km², representing a percentage increase of 76.55 % and built-up increased by 0.944 km², representing a percentage increase of 3.37 %. Vegetation and waterbody experienced a decrease in land area by 9.625 km² and 0.002 km², representing a percentage decrease of 54.56 % and 0.53 % respectively.

Over the entire 29-year (1991-2020) period, a total land area of 15.104 km² (26.34 %) remained unchanged (Table 8). Out of the total unchanged LULC, vegetation had the most (41.48 %) land area remaining the same (i.e., 6.265 km²) while waterbody had the least (0.01 %) land area (i.e., 0.298 km²). The LULC class which lost most land area was vegetation, trading-off land areas of 18.921 km² (47.59 %) and 14.537 km² (36.57 %) to built-up and bare land respectively. Other significant land cover changes experienced were from bare land to built-up and vice versa. That is, bare land traded off a total land area of 4.347 km² (53.30 %) to built-up as built-up traded-off a total of land area of 2.389 km² (27.50 %) to bare land within the same period. The least land area trade-offs experienced was from built-up (0.005 km² (0.06 %)) and bare land (0.007 km² (0.08 %)) to waterbody. Waterbody traded-off land area to all other LULC classes, losing land areas of 0.198 km² (26.60 %) to vegetation; 0.149 km² (20.07 %) to built-up; and 0.099 km² (13.30 %) to bare land. Overall, built-up and bare land recorded gains in land area by 20.272 km² and 11.872 km², representing increase of 233.41 % and 145.58 % respectively. However, vegetation and waterbody experienced decreases in land area by 31.740 km² and 0.404 km², representing a decrease of 79.84 % and 54.29 % respectively.

LULC trends analysis

Over the 29-year period, the trend analysis on land cover changes within the Kpeshie Lagoon Basin revealed changes in all 4 LULC classes. Overall, built-up and bare land recorded massive gains in land area increasing by 20.272 km² (233.41 %) and 11.872 km² (145.58 %) respectively. In contrast, vegetation and waterbody experienced decreases in land area by 31.739 km² (79.84 %) and 0.404 km² (54.29 %) respectively over the same period.

For the various time-steps, bare land gained the most land area between 1991 to 2002 and 2013 to 2020, that is, land areas of 11.221 km² (137.6 %) and 8.683 km² (76.55 %) respectively while built-up gained the most (71.57 %) land area between 2002 to 2013, that is a land area of 11.686 km². Conversely, waterbody suffered the most loss of land area losing more than half (52.96 %) of its land area between 1991 to 2002, that is, a land area of 0.394 km²; then lost a land area of 0.008 km² (2.31 %) between 2002 to 2013; and 0.002 km² (0.53 %) from 2013 to 2020. Table 9 shows the gain and loss of LULC classes for the different time-step.

Overall, built-up experienced a rise in the total land area from 8.685 km² (15.15 %) to 28.957 km² (50.50 %). However, vegetation decreased constantly from 39.754 km² (69.33%) to 8.014 km² (13.98 %). Waterbody also decreased from 0.744 km² (1.30%) to 0.340 km² (0.59 %). Bare land was undulating starting from 8.155 km² (14.22 %) in 1991 and ending at 20.027 km² (34.93 %) in 2020. Built-up and bare land dominated majority of the land area in 2020 as previously dominated by vegetation in 1991. Waterbody covered less land area but also reduced constantly over the period. Figure 4 shows graphical representations of LULC trend analysis from 1991 to 2020.

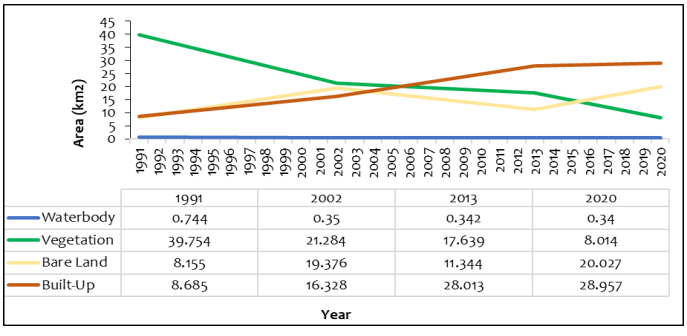

Figure 4 LULC trend analysis of the Kpeshie lagoon basin from 1991 to 2020

Rate of change

Over the 29-year period, built-up recorded the highest rate of change at a rate of 4.24 % while vegetation experienced the worse at a rate of -5.37 %. Within the same period, bare land recorded a positive rate of change at 3.15 % and waterbody recorded a negative rate of change at -2.66 %. The worse rate of change was experienced by vegetation between 2013 to 2020 at a rate of -10.66 % while bare land recorded the highest rate of change at 8.46 % in the same period of time. Other high rate of change was recorded by bare land between 1991 to 2002 at a rate of 8.19%. Built-up recorded high rate of change between 1991 to 2002 and 2002 to 2013 at rates of 5.91 % and 5.03 % respectively. The rate of change of LULC classes between 1991 and 2020 is as presented in Table 10.

Spatial prediction

The predicted LULC map (Figure 5) for the year 2030 showed that majority (60.15 %) of the total land area will be built-up constituting 34.485 km^2 while waterbody will cover the least (0.49 %) covering a land area of 0.282 km^2. Bare land will cover a land area of 18.573 km^2 representing 32.39%. Less than

Table 9 Gain and loss of LULC classes for the different time-step

LULC Class	1991-2002		2002-2013		2013-2020		1991-2020	
	km^2	%	km^2	%	km^2	%	km^2	%
Waterbody	-0.394	-52.96	-0.008	-2.31	-0.002	-0.53	**-0.404**	**-54.29**
Vegetation	-18.470	-46.46	-3.645	-17.13	-9.625	-54.56	**-31.740**	**-79.84**
Bare Land	11.221	137.60	-8.032	-41.46	8.683	76.55	**11.872**	**145.58**
Built Up	7.643	88.00	11.685	71.57	0.944	3.37	**20.272**	**233.41**

Table 10 Rate of change of LULC classes between 1991 and 2020

LULC Class	1991-2002 (%)	2002-2013 (%)	2013-2020 (%)	1991-2020 (%)
Waterbody	-6.63	-0.21	-0.08	**-2.66**
Vegetation	-5.52	-1.69	-10.66	**-5.37**
Bare Land	8.19	-4.75	8.46	**3.15**
Built-Up Area	5.91	5.03	0.47	**4.24**

Table 11 Predicted land area for 2030

LULC Class	Area (km^2)	%
Waterbody	0.282	0.49
Vegetation	3.998	6.97
Bare Land	18.573	32.39
Built-Up Area	34.485	60.15
Total	**57.338**	**100.00**

Table 12 Predicted LULC area and percentage changes from 2020 to 2030

LULC Class	2020 (km^2)	2030 (km^2)	Area Change (km^2)	Percentage Change (%)
Waterbody	0.340	0.282	-0.058	-17.02
Vegetation	8.014	3.998	-4.016	-50.11
Bare Land	20.027	18.573	-1.454	-7.26
Built-Up Area	28.957	34.485	5.528	19.09

one-tenth (6.97 %) of the total land area will be covered by vegetation, that is, a land area of 3.998 km^2 (Table 11).

The spatial predictions showed that vegetation and waterbody will continue to decrease. About 50.11 % of the land area of vegetation in 2020 will be lost; i.e., decreasing from 8.014 km^2 to 3.998 km^2, representing a land area of 4.016 km^2. Waterbody will decrease from 0.340 km^2 in 2020 to 0.282 km^2 by 2030; i.e., a decrease in land area of 0.058 km^2 representing a percentage decrease of 17.02 %. Interestingly, the spatial prediction estimates that bare land will decrease from 20.027 km^2 in 2020 to 18.573 km^2 by 2030. Thus, a decrease in land area of 1.454 km^2, representing a percentage decrease of 7.26 % (Table 12).

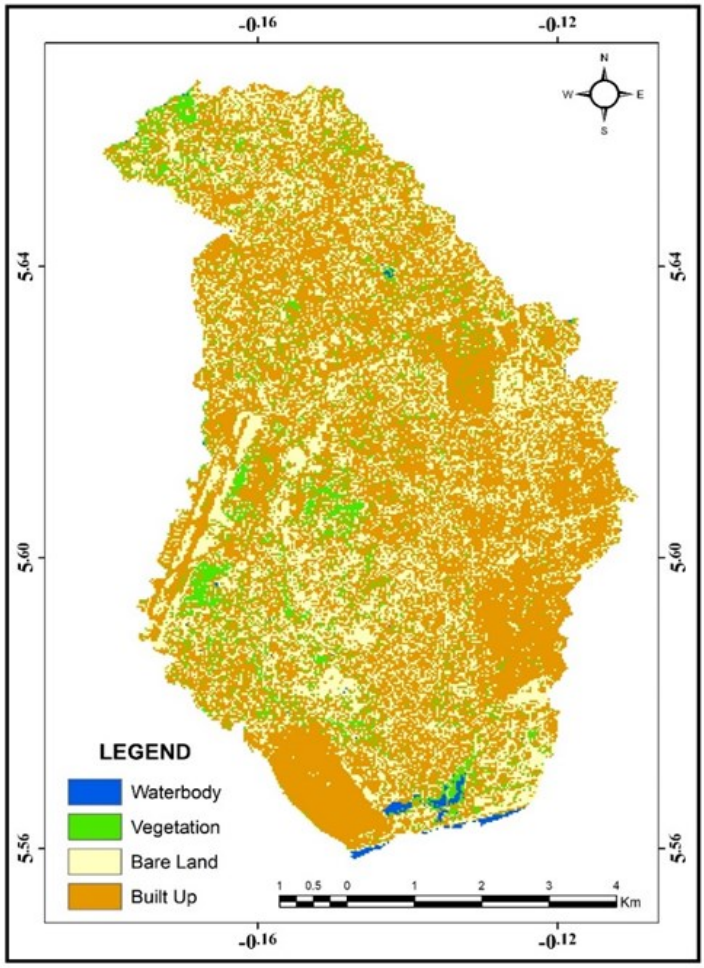

Figure 5 Predicted LULC Map for 2030

Discussion

Within the Kpeshie Lagoon Basin, vegetation was initially the dominant LULC class as it covered majority (69.33 %) of the total land area but overtime built-up area dominated, covering about half (50.50 %) of the total land area of the basin. Bare land also followed suit, increasing from covering 14.22 % of the total land area in 1991 to 34.93 % by 2020. Vegetation and waterbody were identified to be the most vulnerable LULC classes losing 79.84 % and 54.29 % of their initial land area respectively. Consequently, built-up area and bare land gained 233.41 % and 145.58 % of their initial land area respectively. The increase in built-up and bare land coupled with the sharp decline of vegetation and waterbody indicates a high intensity of human activities within the basin affirming the assertion on the trend of vegetation and waterbody being at risk of depletion due to human activities (Yeboah *et al*., 2017). Over the study period, vegetation covered areas owned by institutions namely Burma Camp, Teshie Military Training School and University of Ghana, thereby preserving vegetation within their jurisdiction. Land use planning and development control of most parts of the basin is undertaken by various MMDAs prompting the issues of coordination and sustainability amongst governmental institutions (Odame-Ababio, 2003).

Vegetation was mainly observed along the waterbodies but the massive depletion of vegetation has exposed the waterbody thereby leaving it vulnerable to human activities such as waste disposal into the waterbodies (Quarshie, 2015). This is shown in Figure 2 as bare land and built-up had drawn close to the waterbodies. The massive conversion from vegetation to built-up area can be attributed to the influx of people into the basin due to the pressure for land spaces within Accra and Tema. Similar to many cities and urban areas, Accra and Tema has experienced rapid urbanisation and population growth which are major drivers of LULC changes (Morshed *et al*., 2017) causing a spill over into neighbouring communities, including Teshie, East Legon and Spintex within the Kpeshie Lagoon Basin, as these communities fall between Accra and Tema. Although these communities are planned, they face the challenge of effective implementation (Eduful and Shively, 2015; GWRC, 2012) causing the incidence of flooding in East Legon, Spintex and Teshie communities in recent times. From the 2021 population and housing census (Ghana Statistical Service, 2021), it is evident that there is population growth within the study area. Therefore, it can be concluded that LULC changes within the basin has been influenced by population growth. Since the introduction of Ghana's Zoning Guidelines and Planning Standards (2011) and Riparian Buffer Zone Policy (2013), LULC trends have behaved differently (Table 13). Thus, cumulatively the vulnerable LULC classes, that is, vegetation and waterbody traded off a total land area of 22.5171 km^2 with built-up areas and bare land before the regulations (1991 – 2013) and 9.6282 km^2 after the regulations (2013 – 2020). However, the percentage decrease of vegetation for both were similar, that is, 55.63 % before the regulations and 54.56 % after, that is, above half of vegetation was lost within both eras.

Although built-up area continued increasing, the percentage increase for the period after the introduction of the regulations was far less than before the introduction, that is, 222.55 % before and 3.37 % after the regulation. Comparing the rate of change before and after the introduction of these water-related regulations, waterbody and built-up area were positively impacted while vegetation and bare land were negatively impacted (Table 13). Interestingly, vegetation decreased at a higher rate (-10.66 %) after the introduction of the regulations than it was before (-3.63). Similarly, bare land increase at a higher rate (8.46 %) than before (1.51%). Challenges of enforcement of regulations and ensuring compliance of policies has hindered the implementation of water-related policies (GWRC, 2012; MWRWH, 2014).

The LULC trends observed within the basin revealed that the increase in bare land signals a subsequent increase in built-up areas. Thus, when an area converts to bare land it is most probably in readiness to be built-up. Therefore, it is envisaged that bare land massively gaining a land area of 8.683 km^2 between 2013 to 2020 will propel an increase of built-up by 2030. Thereby, spatial predictions indicate that built-up area will increase by a land area of 5.528 km^2 by 2030.

Conclusion

Image classification made it possible to determine LULC for the Kpeshie Lagoon Basin over a 29-year period (i.e., 1991, 2002, 2013 and 2020). The image classification revealed that vegetation dominated the Kpeshie Lagoon in 1991, covering a

Table 13 LULC trends before and after the implementation of regulations

LULC Class	Before Regulations 1991-2013			After Regulations 2013-2020		
	km^2	%	Rate of Change (%)	km^2	%	Rate of Change (%)
Waterbody	-0.402	-54.05	-3.47	-0.002	-0.53	-0.08
Vegetation	-22.115	-55.63	-3.63	-9.625	-54.56	-10.66
Bare Land	3.189	39.10	1.51	8.683	76.55	8.46
Built-Up Area	19.328	222.55	5.47	0.944	3.37	0.47

land area of 39.754 km^2 (69.33 %). By 2020, approximately half (50.50 %) of the land area (i.e., 28.957 km^2) was coverted to built-up. The massive changes in LULC classes over the study period can be attributed to rapid urbanization due to population growth coupled with LULC policy implementation challenges.

Continuation of the current LULC trend, where vegetation and waterbody decrease while built-up area increases, will expose the vulnerability of the basin to the challenges of climate change. Recommendations for the introduction of Integrated Water Resource Management (IWRM) plans by some researchers to manage water resources yielded results with the introduction of several water related policies and regulations. However, implementation of these policies has not been effective as there are incidents of the negative effects of human activities on waterbodies and vegetation.

Acknowledgement

The authors are grateful to the anonymous reviewers for their comments, which helped to improve this work.

Conflicts of Interest Declaration

The authors declare no conflict of interest.

References

Aksoy, E., Özsoy, G. and Dirim, M. S. (2009). Soil mapping approach in GIS using Landsat satellite imagery and DEM data. African Journal of Agricultural Research, 4 (11), pp. 1295–1302. http://www.academicjournals.org/AJAR

Amoako, C. and Boamah, E.F. (2015). The three-dimensional causes of flooding in Accra, Ghana. International Journal of Urban Sustainable Development 7:1, pp. 109 – 129.

Aneesha, S. B., Shashi, M., and Deva, P. (2020). Future land use land cover scenario simulation using open source GIS for the city of Warangal, Telangana, India. Applied Geomatics, 12(3), pp. 281–290. https://doi.org/10.1007/s12518-020-00298-4

Apau, J., Appiah, S., and Marmon-Halm, M. (2012). Assessment of water quality parameters of Kpeshie Lagoon of Ghana. Journal of Science and Technology (Ghana), 32(1). https://doi.org/10.4314/just.v32i1.4

Asare, Y. M., Forkuo, E. K., Forkuor, G., and Thiel, M. (2020). Evaluation of gap-filling methods for Landsat 7 ETM+ SLC-off image for LULC classification in a heterogeneous landscape of West Africa. International Journal of Remote Sensing, 41(7), pp. 2544–2564. https://doi.org/10.1080/01431161.2019.1693076

Ayivor, J. S. and Gordon, C. (2012). Impact of land use on river systems in Ghana. West African Journal of Applied Ecology, 20(3 SPL. EDN), pp. 83–95. https://doi.org/10.4314/wajae.v20i3

Azabdaftari, A., and Sunar, F. (2016). Soil Salinity mapping using multitemporal Landsat data. The International Archives of the Photogrammetry, Remote Sensing and Spatial Information Sciences, XLI-B7. https://doi.org/10.5194/isprsarchives-XLI-B7-3-2016

Boampong, J. N. (2020). An assessment of land use/landcover and shoreline changes in the coastal zone of Greater Accra region, Ghana (UiT The Arctic University of Norway). https://munin.uit.no/bitstream/handle/10037/19345/thesis.pdf?sequence=2

Breiman, L. (2001). Random forests. Machine Learning, pp. 45 (1), 5–32. https://doi.org/10.1023/A:1010933404324

Congalton, R. G. (1991). A review of assessing the accuracy of classifications of remotely sensed data. Remote Sensing of Environment, 37(1), pp. 35–46. https://doi.org/10.1016/0034-4257(91)90048-B

Cotillon, S.E., 2017, West Africa land use and land cover time series: U.S. Geological Survey Fact Sheet 2017–3004, 4 p., https://doi.org/10.3133/fs20173004.

Coulter, L. L., Stow, D. A., Tsai, Y. H., Ibanez, N., Shih, H. C., Kerr, A., Weeks, J. R., and Mensah, F. (2016). Classification and assessment of land cover and land use change in southern Ghana using dense stacks of Landsat 7 ETM+ imagery. Remote Sensing of Environment, 184 (August), pp. 396–409. https://doi.org/10.1016/j.rse.2016.07.016

Dewan, A. M., Yamaguchi, Y. (2009). Land use and land cover change in Greater Dhaka, Bangladesh: Using remote sensing to promote sustainable urbanization. Applied Geography 29, pp. 390–401.

Eduful, M., and Shively, D. (2015). Perceptions of urban land use and degradation of water bodies in Kumasi, Ghana. Habitat International, 50, pp. 206–213. https://doi.org/10.1016/j.habitatint.2015.08.034

Esteve, P., Fontes, J., and Gastellu-Etchegorry, J. P. (1998). Tropical dry ecosystems modelling and monitoring from space. Ecological Modelling, 108, pp. 175–188. Retrieved from https://www.researchgate.net/publication/237100479

European Environment Agency (EEA), (2008). Progress towards halting the loss of biodiversity by 2010. EEA Report pp. 1–104

Forkuor, G., Conrad, C., Thiel, M., Ullmann, T., and Zoungrana, E. (2014). Integration of optical and synthetic aperture radar imagery for improving crop mapping in northwestern Benin, West Africa. Remote Sensing, 6(7), pp. 6472–6499. https://doi.org/10.3390/rs6076472

Forkuor, G., Dimobe, K., Serme, I., and Tondoh, E. J. (2017a). Landsat-8 vs . Sentinel-2 : examining the added value of sentinel-2 ' s red-edge bands to land-use and land-cover

mapping in Burkina Faso. GIScience and Remote Sensing, pp. 1–24. https://doi.org/10.1080/15481603.2017.1370169

Forkuor, G., Hounkpatin, O. K. L., Welp, G., and Thiel, M. (2017b). High resolution mapping of soil properties using remote sensing variables in south-western Burkina Faso : A comparison of machine learning and multiple linear regression models. PLoS ONE, 12(1), e0170478. https://doi.org/10.1371/journal.pone.0170478

Friedman, J. H. (2002). Stochastic gradient boosting. Computational Statistics and Data Analysis 38 (4), pp. 367–378. doi:10.1016/S0167-9473(01)00065-2

Ghana Statistical Service (2014). 2010 Population and housing census. District Analytical Report, Adentan Municipality. https://www2.statsghana.gov.gh/docfiles/2010_District_Report/ (Accessed on 21/02/20)

Ghana Statistical Service (2021). 2021 Population and housing census general report, Volume 3A. Population of Regions and Districts**.** https://census2021.statsghana.gov.gh/bannerpage.php?readmorenews=MTQ1MTUyODEyMC43MDc1and 2021-PHC-General-Report. (Accessed on 20/01/2022)

Ghana Water Resources Commission (GWRC) (2012). National integrated water resources management (IWRM) plan, Ghana Water Resources Commission. http://doc.wrc-gh.org/pdf/National%20IWRM%20Plan.pdf (Accessed on 13/05/2019)

Ghansah, B., Asare, Y. M., Tchao, E. T., and Forkuo, E. K. (2016). Mapping the spatial changes in Lake Volta using multitemporal remote sensing approach. Lakes and Reservoirs: Research and Management, 21, pp. 206–215. https://doi.org/10.1111/lre.12138

Gong, P., Wang, J., Yu, L., Zhao, Y., Zhao, Y., Liang, L., … Chen, J. (2013). Finer resolution observation and monitoring of global land cover : first mapping results with Landsat TM and ETM + data. International Journal of Remote Sensing, 34(7), pp. 2607–2654. https://doi.org/10.1080/01431161.2012.748992

Hellweger, F. L., Schlosser, P., Lall, U., and Weissel, J. K. (2004). Use of satellite imagery for water quality studies in New York Harbor. Estuarine, Coastal and Shelf Science, 61, pp. 437–448. https://doi.org/10.1016/j.ecss.2004.06.019

Hu, T., Yang, J., Li, X., and Gong, P. (2016). Mapping urban land use by using landsat images and open social data. Remote Sensing, 8, 151. https://doi.org/10.3390/rs8020151

Kamaraj, M., and Rangarajan, S. (2022). Predicting the future land use and land cover changes for Bhavani basin, Tamil Nadu, India, using QGIS MOLUSCE plugin. Environmental Science and Pollution Research. https://doi.org/10.1007/s11356-021-17904-6

Laili, N., Arafah, F., Jaelani, L. M., Subehi, L., Pamungkas, A., Koenhardono, E. S., and Sulisetyono, A. (2015). Development of water quality parameter retrieval algorithms for estimating total suspended solids and chlorophyll-a concentration using Landsat-8 imagery at poteran island water. ISPRS Annals of the Photogrammetry, Remote Sensing and Spatial Information Sciences, II-2/W2. https://doi.org/10.5194/isprsannals-II-2-W2-55-2015

Leslie, B. C. R., Serbina, L. O., and Miller, H. M. (2017). Landsat and agriculture — case studies on the uses and benefits of landsat imagery in agricultural monitoring and production. https://doi.org/10.3133/ofr20171034

Loveland, T. R., and Dwyer, J. L. (2012). Landsat : building a strong future. Remote Sensing of Environment, 122, pp. 22–29. https://doi.org/10.1016/j.rse.2011.09.022

Lu, D., Tian, H., Zhou, G., and Ge, H. (2008). Regional mapping of human settlements in southeastern China with multisensor remotely sensed data. Remote Sensing of Environment, 112, pp. 3668–3679. https://doi.org/10.1016/j.rse.2008.05.009

Lunetta, R. S., Knight, J. F., Ediriwickrema, J., Lyon, J. G., and Dorsey, L. (2006). Land-cover change detection using multi-temporal MODIS NDVI data land-cover change detection using multi-temporal. Environmental Protection, 43(1), pp. 142–154. https://doi.org/16/j.rse.2006.06.018

Merem, E. C., Twumasi, Y., Wesley, J., Isokpehi, P., Shenge, M., Fageir, S., … Nwagboso, E. (2017). Assessing the ecological effects of mining in West Africa : The case of Nigeria. International Journal of Mining Engineering and Mineral Processing, 6(1), pp. 1–19. https://doi.org/10.5923/j.mining.20170601.01

Ministry of Water Resources Works and Housing (MWRWH). (2014). Water sector strategic development plan (2012-2025). https://www.wrc-gh.org/documents/reports/. (Accessed on 21/02/20).

Morshed, N., Yorke, C., and Zhang, Q. (2017). Urban expansion pattern and land use dynamics in Dhaka, 1989–2014. Professional Geographer, 69(3), pp. 396–411. https://doi.org/10.1080/00330124.2016.1268058

Mountrakis, G., Im, J., and Ogole, C. (2011). Support vector machines in remote sensing: a review. ISPRS Journal of Photogrammetry and Remote Sensing 66 (3), pp. 247–259. doi:10.1016/j.isprsjprs.2010.11.001.

Nawar, S., Buddenbaum, H., Hill, J., and Kozak, J. (2014). Modeling and mapping of soil salinity with reflectance spectroscopy and Landsat data using two quantitative methods (PLSR and MARS). Remote Sensing, 6, pp. 10813–10834. https://doi.org/10.3390/rs61110813

NextGIS. (2013). MOLUSCE - quick and convenient analysis of land cover changes. https://nextgis.com/blog/molusce/ (Accessed on 22/12/2020).

Odame-Ababio, K. (2003). Putting integrated water resource management in practice - Ghana's experience. Proceedings of the African Regional Workshop on Water Management, Nairobi, Kenya. http://colinmayfield.com/public/PDF_files/IWRM_GHANA%E2%80%99S%20EXPERIENCE.pdf (Accessed on 18/04/2019)

Onojeghuo, A. O., and Onojeghuo, A. R. (2015). Mapping forest transition trends in Okomu reserve using Landsat and UK-DMC-2 satellite data. South African Journal of Geomatics, 4(4), 486–501. https://doi.org/10.4314/sajg.v4i4.9

Organisation for Economic Co-operation and Development (OECD). Monitoring land cover change. Retrieved from http://www.oecd.org/env/indicators-modelling-outlooks/monitoring-land-cover-change.html (Accessed on 26/01/2020).

Pandit, S. (2011). Forest cover and land use change: A Study of Laljhadi Forest (Corridor, Far Western Development Region, Nepal, MSc. Thesis, Tribhuvan University

Poorter, L., Bongers, F., Kouame, F. N., and Hawthorne, W. (2004). Biodiversity of West African forests : an ecological atlas of woody plant species biodiversity of West African forests - an ecological atlas of woody plant species. https://doi.org/10.1079/9780851997346.0041

Quarshie J. T. (2015). Assessment of litter on the banks of some selected lagoons along the eastern Coast of Ghana. http://ugspace.ug.edu.gh. (Accessed on 19/11/19)

Roy, D. P., Ju, J., Mbow, C., Frost, P., Loveland, T., Roy, D. P., … Loveland, T. (2017). Accessing free Landsat data via the Internet : Africa's challenge. Remote Sensing

Letters, 1(2), pp. 111–117. https://doi.org/10.1080/01431160903486693

Smits, P. C., Dellepiane, S. G., and Schowengerdt, R. A. (1999). Quality assessment of image classification algorithms for land-cover mapping: A review and a proposal for a cost-based approach. International Journal of Remote Sensing, 20(8), pp. 1461–1486. https://doi.org/10.1080/014311699212560

Stefanski, J., Kuemmerle, T., Chaskovskyy, O., Griffiths, P., Havryluk, V., Knorn, J., … Waske, B. (2014). Mapping land management regimes in western Ukraine using optical and SAR data. Remote Sensing, 6, pp. 5279–5305. https://doi.org/10.3390/rs6065279

Tom-Dery, D., Dagben, Z. J., and Cobbina, S. J. (2012). Effect of illegal small-scale mining operations on vegetation cover of arid. Research Journal of Environmental and Earth Sciences, 4(6), pp. 674–679. http://maxwellsci.com/print/rjees/v4-674-679.pdf

Torbick, N., Chowdhury, D., Salas, W., and Qi, J. (2017). Monitoring rice agriculture across Myanmar using time series Sentinel-1 assisted by Landsat-8. Remote Sensing, 9, 119. https://doi.org/10.3390/rs9020119

United Nations, Department of Economic and Social Affairs, Population Division (2019). World population prospects 2019, Online Edition. Rev. 1. https://population.un.org/wpp/Download/Standard/Population/. (Accessed on 25/01/2020).

Vittek, M., Brink, A., Donnay, F., Simonetti, D., and Desclé, B. (2014). Land cover change monitoring using Landsat MSS/TM satellite image data over West Africa between 1975 and 1990. Remote Sensing, 6, pp. 658–676. https://doi.org/10.3390/rs6010658

White, J. C., Wulder, M. A., Hermosilla, T., Coops, N. C., and Hobart, G. W. (2017). A nationwide annual characterization of 25 years of forest disturbance and recovery for Canada using Landsat time series. Remote Sensing of Environment, 194, pp. 303–321. https://doi.org/10.1016/j.rse.2017.03.035

Yadav, P. K., Kapoor, M., and Sarma, K. (2012). Land use land cover mapping, change detection and conflict analysis of Nagzira-Navegaon Corridor, Central India using geospatial technology. International Journal of Remote Sensing and GIS, pp. 90–98.

Yeboah, F., Awotwi, A., Forkuo, E. K., and Kumi M. (2017). Assessing the land use and land cover changes due to urban growth in Accra, Ghana. Journal of Basic and Applied Research International 22(2), pp. 43-50

Zurqani, H. A., Post, C. J., Mikhailova, E. A., Schlautman, M. A., and Sharp, J. L. (2018). Geospatial analysis of land use change in the Savannah River Basin using Google Earth Engine. International Journal of Applied Earth Observation and Geoinformation 69, pp. 175–185. https://doi.org/10.1016/j.jag.2017.12.006